Enhanced luminous efficiency of phosphor-converted LEDs by using back reflector to increase reflectivity for yellow light

Shengjun Zhou,[1,2] Bin Cao,[1] Shu Yuan,[3] and Sheng Liu[1,*]

[1]School of Power and Mechanical Engineering, Wuhan University, Wuhan 430072, China

[2]School of Mechanical Engineering, Shanghai Jiao Tong University, Shanghai 200240, China

[3]Quantum Wafer Inc., Foshan 528251, China

*Corresponding author: victor_liu63@126.com

Received 25 August 2014; revised 29 October 2014; accepted 29 October 2014;
posted 31 October 2014 (Doc. ID 221651); published 25 November 2014

To obtain high reflectivity over a broad range of green, yellow, and red light as well as blue light incidents from a particular angular range and further increase the luminous efficiency of a phosphor-converted white LED packaging module, a novel back hybrid reflector including a SiO_2 total internal reflection layer (TIR), five-pair SiO_2/TiO_2 double distributed Bragg reflector (DBR) stacks, and a gold (Au) metallic mirror was designed and fabricated. The double DBR stacks have layers configured to reflect green, yellow, and red light as well as blue light, which includes a first portion where the thickness of the layers are relatively larger, and also includes a second portion where the thickness of the layers is relatively smaller. Light that is passing toward the hybrid reflector at angles greater than the critical angle (56°) is reflected by the SiO_2 TIR layer at the sapphire/SiO_2 interface, whereas the light that passes through the SiO_2 TIR layer with incident angles between 0° and 56° is reflected by the double DBR stacks. The overall hybrid reflector can ensure a reflectivity of more than 95% in both the blue light wavelength region and the yellow light wavelength region. The obtained higher reflectivity in the yellow light wavelength region will benefit the phosphor-converted LEDs because yellow light backscattered by phosphor particles is reflected upward.

OCIS codes: (230.0230) Optical devices; (230.3670) Light-emitting diodes.
http://dx.doi.org/10.1364/AO.53.008104

1. Introduction

Light-emitting diodes (LEDs), based on III-nitride semiconductors, have been regarded as the next generation of lighting sources because of their potential advantages such as high efficiency, long lifetime, and high reliability [1–4]. Despite the rapid development of GaN-based LEDs, the light extraction efficiency (LEE) of LEDs grown on a sapphire substrate is still an important obstacle due to the small light escape cone caused by the large refractive index difference between GaN and air [5–7]. The light absorption caused by a GaN semiconductor and metal electrode can also decrease the LEE of LEDs [8,9]. The InGaN/GaN multiple quantum well (MQW) active layer of the blue LED chip emits light in all directions, and the light bounces randomly within the LED chip. A substantial amount (about 50%) of light travels downward, which does not contribute to useable light output. Accordingly, increasing the reflectivity of the bottom surface of a sapphire substrate by employing a back reflector to reflect the light that travels downward is a potential way to improve the LEE of LEDs. The back reflector can be a single highly reflective metallic mirror such as aluminum (Al) and silver

1559-128X/14/348104-07$15.00/0

(Ag) [10]. Although a metallic mirror has a high reflectivity over a broad range of frequencies incident from arbitrary angles, it suffers from poor mechanical adhesion with a sapphire substrate. An adhesion layer of chromium (Cr) must be sandwiched between the metallic mirror and the sapphire substrate, reducing the reflectivity of the metallic mirror. As an alternative approach to a metallic mirror, multilayer dielectric mirrors such as a distributed Bragg reflector (DBR) or an omni-directional reflector (ODR), used primarily to reflect a narrow range of frequencies incident from a particular angular range, have also been employed to serve as the LED back reflector [11–13]. Although the previously reported single DBR or ODR stack designed for a blue LED chip has obtained high reflectivity in the blue light wavelength region, it exhibited low reflectivity in the green, yellow, or red light wavelength region.

For commercially available phosphor-converted LEDs (pc-LEDs), phosphor particles are often dispersed in a silicone matrix and then directly or indirectly coated on the blue LED chip. The phosphor particles absorb a fraction of the blue light emanating from the LED chip and downconvert, thereby reemitting light of longer wavelength including green, yellow, and red light. The remaining fraction of blue light can be transmitted through the phosphor silicone gel layer by the scattering of phosphor particles. The downconverted light can propagate in the top direction or in the opposite direction due to backscattering by phosphor particles [14]. The transmitted blue light and the downconverted yellow light generate white light by color mixing, which is useable light output from pc-LEDs for general lighting. Hence, the low reflectivity of the LED back reflector employing a conventional single DBR stack in the green, yellow, or red light wavelength regions may decrease the luminous efficiency of pc-LEDs.

To overcome the disadvantage of the single DBR stack and further increase the luminous efficiency of pc-LEDs, a novel back hybrid reflector including a SiO_2 total internal reflection (TIR) layer, double DBR stacks, and a Au metallic mirror, optimized to ensure high reflectivity in green, yellow, and red light as well as blue light, was proposed and demonstrated in this paper.

2. Experiments

An LED epitaxial layer was grown on a patterned sapphire substrate (PSS) by metal organic chemical vapor deposition (MOCVD) equipment. Trimethylgallium (TMGa), trimethylindium (TMIn), and ammonia (NH_3) were used as precursors. Silane (SiH_4) and biscyclopentadienymagnesium (Cp_2Mg) were used as the n-dopant and p-dopant source. The LED epitaxial layer consists of a 30 nm thick GaN nucleation layer, a 1.5 μm thick undoped GaN buffer layer, a 3 μm thick Si-doped n-GaN layer, a InGaN/GaN multiple quantum well (MQW), a 100 nm thick Mg doped p-AlGaN electron blocking layer, and a 190 nm thick Mg-doped p-GaN layer. The InGaN/GaN MQW structure consists of twelve pairs of 3 nm thick $In_{0.16}Ga_{0.84}N$ well layers and a 12 nm thick GaN barrier layer. After the epitaxial growth process, the LED wafer was subsequently annealed at 750°C in a N_2 atmosphere to activate Mg in the p-GaN layer.

An inductively coupled plasma etching process was used to etch the mesh structure of the LED in order to expose the n-GaN semiconductor layer. The indium-tin oxide (ITO) layer with thickness of 230 nm was deposited on the p-GaN surface as the current spreading layer using electronic beam evaporator. The LED wafer was then rapid thermal annealed at 540°C for 10 min in nitrogen ambient to improve ohmic contact performance between the ITO and p-GaN layer. A Cr/Pt/Au (50 nm/50 nm/1.5 μm) was deposited on the top of the LED as an n-electrode and p-electrode, respectively. The LED wafer was thinned down to be about 100 μm thick by grinding and polishing. In order to investigate the effect of a DBR stack on the luminous efficiency of pc-LEDs packaging modules, different structures of DBR stacks comprising an array of alternating SiO_2/TiO_2 dielectric layers were deposited on the bottom of the polished sapphire substrate. Finally, the LED wafer was diced into chips with size of 1 mm × 1 mm. The LED chip with a ten-pair single SiO_2/TiO_2 DBR stack (LED A), the LED chip with ten-pair double SiO_2/TiO_2 DBR stacks (LED B), and the LED chip with a hybrid reflector combining five-pair double SiO_2/TiO_2 DBR stacks and a Au metallic mirror (LED C) was fabricated, respectively. For LED packaging, the blue LED chip (LED A, LED B, and LED C) was attached to a lead frame with adhesive, and the gold wire bonding process was used to provide electrical interconnection. The phosphor silicone gel layer was conformal-coated on the surface of the blue LED chip. The luminous flux of phosphor-converted white LED packaging module (pc-LED A, pc-LED B, and pc-LED C) was measured by using an integrating sphere.

3. Theoretical Model

The DBR is a multilayer structure comprising an array of alternating dielectric layers with high (H) and low (L) refractive indices, which are often made by stacking layers of dielectrics with quarter-wave thickness ($\lambda/4n$, where λ is the central wavelength of the reflectivity spectrum) that rely on thin-film interference [15],

$$n_H t_H = n_L t_L = \lambda/4, \tag{1}$$

where n_H, n_L, t_H, and t_L are the refractive indices and the thicknesses of the alternating dielectric layers, respectively. The thin-film interference effect is typically sensitive to the angle of incidence. The DBR has a high reflectivity within a finite range of frequencies known as the stop band. By engineering the DBR stacks, we can create an LED back reflector

with high reflectivity at visible frequencies incident from a particular angular range.

Figure 1(a) shows a schematic illustration of the simulation model for the reflectivity spectrum of a GaN-based LED chip with a back reflector. To further analyze the effect of the reflectivity of the DBR over yellow light and blue light on the LEE of pc-LEDs, we built the model of a pc-LEDs packaging module, as shown in Fig. 1(b). The 100 μm thick phosphor silicone gel layer in Fig. 1(b) was coated on the surface of the LED chip by the conformal coating method, leading to the uniform thickness of phosphor layer on the top and side surfaces of the LED chip. The blue light is incident upon the DBR from the MQW active layer of the LED chip, and the DBR reflects the blue light that travels downward. The reflected blue light then escapes from the LED chip and reaches the phosphor silicone gel layer. The phosphor absorbs some of the blue light and fluoresces, re-emitting light of longer wavelengths including red, yellow, and green light. The rest of the blue light can be transmitted through the phosphor layer by the scattering of phosphor particles. Therefore, the total spectrum of light emitted from the pc-LEDs packaging module is white light by color mixing. In this model, the refractive indices and absorption coefficients for p-GaN, MQW, and n-GaN were 2.45, 2.54, 2.42, and 5 mm^{-1}, 8 mm^{-1}, 5 mm^{-1}, respectively, [16,17]. The absorption and scattering coefficients of phosphor were 3.18 mm^{-1} and 5.35 mm^{-1} for blue light and 0.03 mm^{-1} and 7.74 mm^{-1} for yellow light [18,19]. For modeling the light conversion process, the rays of blue and yellow light were simulated separately by the Monte Carlo ray tracing method.

The LEE of pc-LEDs for blue light, yellow light, and white light versus the reflectivity of DBR over blue light and yellow light was shown in Fig. 2. While it is assumed that the reflectivity of a DBR over yellow light is 100%, the LEE of pc-LEDs for blue light was increased from 12.7% to 18.9%, the LEE of pc-LEDs for yellow light was increased from 20.4% to

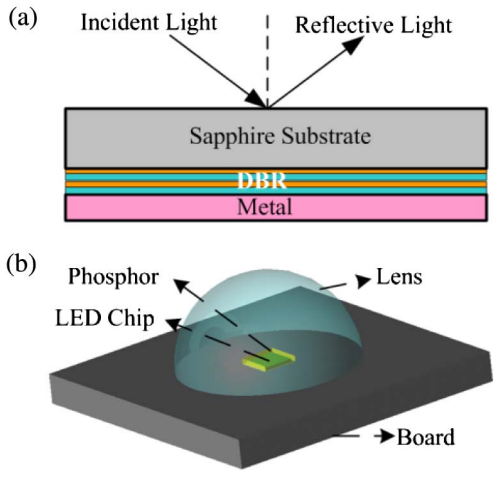

Fig. 1. (a) Schematic illustration of the simulation model for the reflectivity spectrum of a GaN-based LED chip with back reflector and (b) schematic illustration of pc-LEDs packaging module.

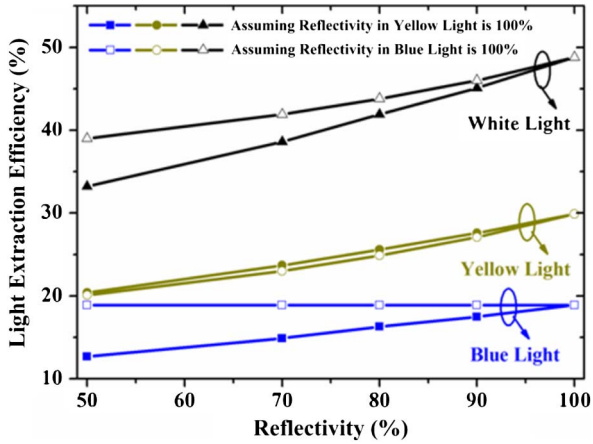

Fig. 2. LEE of pc-LEDs for blue light, yellow light, and white light versus the reflectivity of a DBR over blue light and yellow light.

29.9%, and the total LEE of pc-LEDs for while light was increased from 33.1% to 48.8% when the reflectivity of a DBR over blue light was increased from 50% to 100%. While it is assumed that the reflectivity of a DBR over blue light is 100%, the LEE of pc-LEDs for blue light was kept constant (18.9%), the LEE of pc-LEDs for yellow light was increased from 20.1% to 29.9%, and the total LEE of pc-LEDs for white light was increased from 39% to 48.8% when the reflectivity of a DBR over yellow light was increased from 50% to 100%, as shown in Fig. 2.

Table 1 summarizes the effect of the reflectivity of a DBR over yellow light and blue light on the total LEE of pc-LEDs for white light. Accordingly, an optimized DBR stack design to ensure a reflectivity of more than 95% in both the blue light wavelength region and the yellow light wavelength region can play a critical role in improving the total LEE of pc-LEDs for while light, thus increasing the luminous efficiency of pc-LEDs.

4. Results and Discussion

We used the commercial software, *TFCalc*, to model the design of a DBR stack that was made of thin layers of materials with different dielectric constants (SiO_2 and TiO_2). In our simulation, the refractive indices of the SiO_2/TiO_2 dielectric layers were fixed at 1.47/2.5, and the thicknesses of the SiO_2/TiO_2 DBR stack were fixed at 78.2 nm/45.8 nm. To evaluate the angular dependence of a single DBR stack, we

Table 1. Effect of Reflectivity of a DBR Over Yellow Light and Blue Light on the Total LEE of pc-LEDs

Reflectivity	100%/50% (yellow/blue)	100%/50% (blue/yellow)	100%/100% (blue/yellow)
LEE of pc-LEDs for blue light	12.7%	18.9%	18.9%
LEE of pc-LEDs for yellow light	20.4%	20.1%	29.9%
LEE of pc-LEDs for white light	33.1%	39%	48.8%

compared the simulated reflectivity spectrum for incident angles from 0° to 60°. The change in the reflectivity spectrum and the associated bandwidth of reflectance band at different incident angles for a central wavelength, λ, of 460 nm were shown in Fig. 3. It was noted from Fig. 3 that the bandwidth of the reflectance band with a high reflectivity (>90%) region for the single DBR stack including quarter wavelength layers of SiO_2/TiO_2 can reach up to 140 nm. However, the reflectivity of the single DBR stack, as shown in Fig. 3, exhibited a large angular dependency. As the incident angle of light was increased, the center of the reflectance band was shifted to shorter wavelength (blueshifted) and the bandwidth of the reflectance band was narrowed. This reflectance behavior of the single DBR stack is in good agreement with theoretical dispersion curves and the previous investigation for quarter-wave dielectric stacks [20–23].

The reflectivity spectrum of the single DBR stack optimized for a different central wavelength, λ, by altering the thickness of TiO_2/SiO_2 dielectric layers was shown in Fig. 4. As the thickness of the TiO_2/SiO_2 dielectric layers was increased, the reflective bandwidth of the single DBR stack was redshifted. The redshift toward the long wavelength for the single DBR stack with increasing thickness of TiO_2/SiO_2 dielectric layers can counteract the blueshift toward the short wavelength when the light incident angle increased from the surface normal toward the grazing angle to the DBR stack.

Thus, to maximize the redirection of all emitted photons upward, we combined two single DBR stacks, each optimized for a different central wavelength, λ, into double DBR stacks. The first DBR stack contained five-pair TiO_2/SiO_2 (57.3 nm/98.1 nm) dielectric layers optimized for central wavelength at 560 nm. The second DBR stack included another five-pair TiO_2/SiO_2 (45.8 nm/78.5 nm) dielectric layers optimized for central wavelength at 460 nm. Thus, taking an angle-induced blueshift into account, the double DBR stacks structure should be efficient

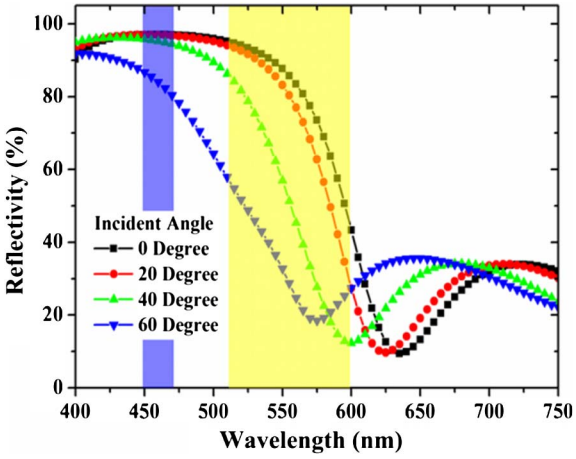

Fig. 3. Reflectivity spectrum of single DBR stack for different angles of light incidence.

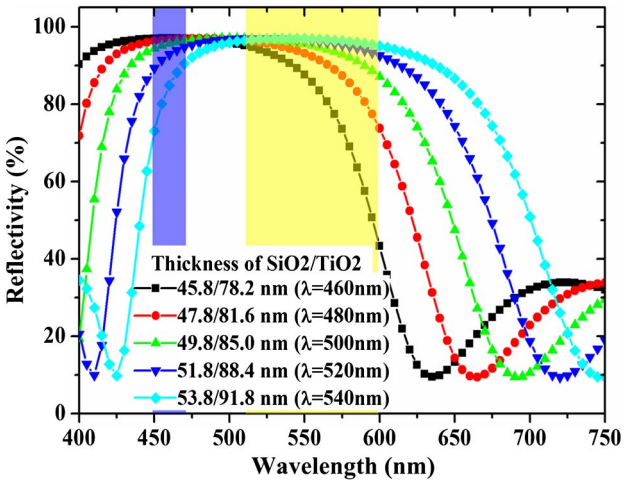

Fig. 4. Reflectivity spectrum of a single DBR stack designed for different central wavelengths.

in both the blue wavelength region and the yellow wavelength region.

Figure 5 compared the normal-incident reflectivity spectrum of the ten-pair TiO_2/SiO_2 single DBR stack to that of the ten-pair TiO_2/SiO_2 double DBR stacks. In order to compare the reflectivity in the blue and yellow wavelength regions, the ranges of the blue and yellow light with bandwidth of 20 and 90 nm were colored [24]. As shown in Fig. 5, the reflectivity of the ten-pair TiO_2/SiO_2 (45.8 nm/78.5 nm) single DBR stack in the blue wavelength region was nearly 100%, whereas it exhibited low reflectivity in the yellow wavelength region. The reflectivity of the ten-pair TiO_2/SiO_2 (57.3 nm/98.1 nm) single DBR stack in the yellow wavelength region was nearly 100%, whereas the reflectivity in the blue light wavelength was low. Compared to the ten-pair single DBR stack, it was revealed from Fig. 5 that the ten-pair double DBR stacks, which included a first five-pair TiO_2/SiO_2 (57.3 nm/98.1 nm) DBR stack and a

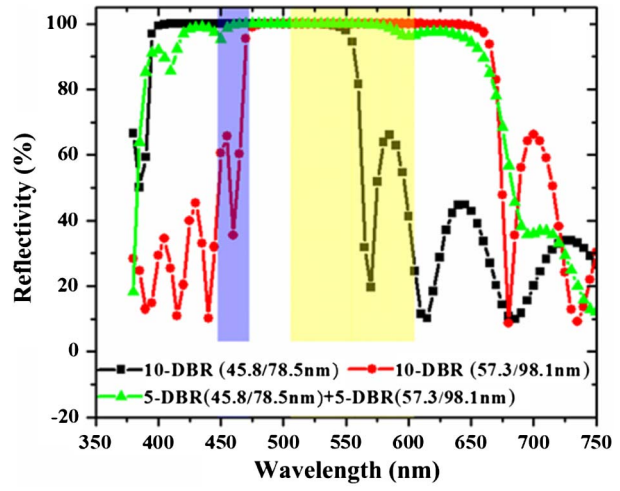

Fig. 5. Comparison of reflectivity spectrum for a ten-pair single DBR stack and ten-pair double DBR stacks at a normal incident angle.

second five-pair TiO_2/SiO_2 (45.8 nm/78.5 nm) DBR stack, exhibited high reflectivity in both the blue wavelength region and the yellow wavelength region.

Figure 6 shows the reflectivity spectrum of the ten-pair double DBR stacks versus the different angles of incidence of light. In contrast to the single DBR stack, it was shown that the bandwidth of the reflectance band with high reflectivity (>90%) using the double DBR stacks may be extended, which was consistent with Southwell's conclusion. It was demonstrated from Southwell's work that the omnidirectional bandwidth of quarter-wave dielectric stacks may be extended by the addition of contiguous quarter-wave dielectric stacks [21]. By varying the dielectric layer thicknesses to compensate for the angular dependence of reflection, the reflectivity spectrum of the double DBR stacks, which may obtain high reflectivity in both the blue wavelength region and the yellow wavelength region over a broad range of incident angles, showed less dependence on incident angles of light compared to the single DBR stack.

Figure 7 showed the SEM image of the fabricated ten-pair double DBR stacks that were deposited on the bottom of the sapphire substrate using the e-beam evaporation system. As shown in Fig. 7, the deposited ten-pair double DBR stacks included a first five-pair TiO_2/SiO_2 DBR stack with thicknesses of each period was 57.3 nm/98.1 nm and a second five-pair TiO_2/SiO_2 DBR stack with thicknesses of each period of 45.8 nm/78.5 nm.

To increase the reflectivity of the DBR, we need to increase the number of pairs of the DBR, which is material and time consuming. If we combine the DBR and metallic mirror, we should be able to achieve a high reflectivity while reducing the number of DBR pairs, thus shortening the process time. The hybrid reflector by combining DBR and Al or Ag has been proposed to provide a superior reflective characteristic and decrease the dependence of the reflectivity spectrum on incident angle of light [25–27].

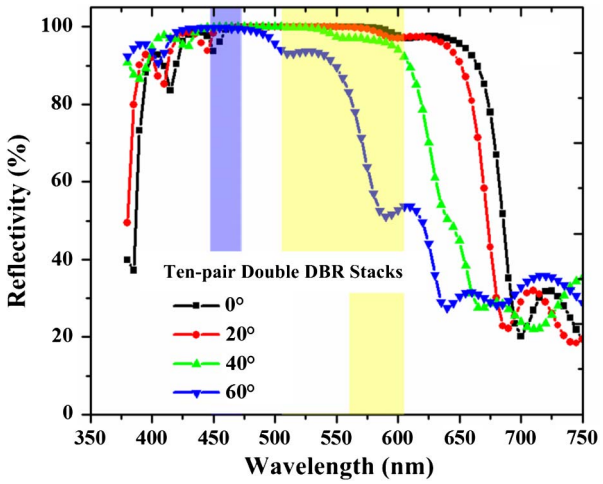

Fig. 6. Reflectivity spectrum of the ten-pair double DBR stacks for different angles of light incidence.

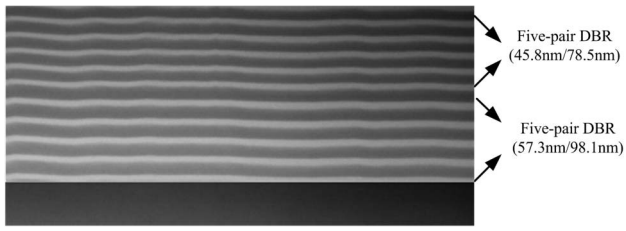

Fig. 7. SEM image of the ten-pair double DBR stacks deposited on the bottom of the sapphire substrate.

It was found that LEDs with a hybrid reflector combing the DBR and Ag showed higher light output power than LEDs with a hybrid reflector combining the DBR and Al, due to the higher reflectivity of Ag [27]. However, Ag is easy to tarnish in the presence of sulfides, chlorides, and oxides in the atmosphere [28]. Gold (Au) is rarely used to form the hybrid reflector due to relatively low reflectivity in the visible light region. However, Au is more chemically stable compared with other metals such as Al and Ag. To overcome the disadvantage of the low reflectivity of Au, we combined five-pair double DBR stacks and a Au metallic mirror to improve the reflectivity of the hybrid reflector.

Figure 8 shows the SEM image of the fabricated hybrid reflector including a SiO_2 TIR layer, five-pair TiO_2/SiO_2 double DBR stacks, and a Au metallic mirror. As shown in Fig. 8, the upper SiO_2 TIR layer had a thickness of 535 nm. The five-pair double DBR stacks consisted of a first DBR stack and a second DBR stack. The first DBR stack included two periods, where each period had a first layer of TiO_2 that was 76.9 nm thick and a second layer of SiO_2 that was 139.5 nm thick. The second DBR stack included three periods, where each period had a first layer of TiO_2 that was 48.9 nm thick and a second layer of SiO_2 that was 90.9 nm thick. An intermediate binding layer of Cr was used to improve adhesion stability between the double DBR stacks and a Au metallic mirror. When light is striking the sapphire ($n_{sapphire} = 1.78$)/SiO_2 ($n_{SiO_2} = 1.47$) interface, the critical angle of TIR is 56° at the interface. Consequently, the SiO_2 TIR layer is used to reflect the light

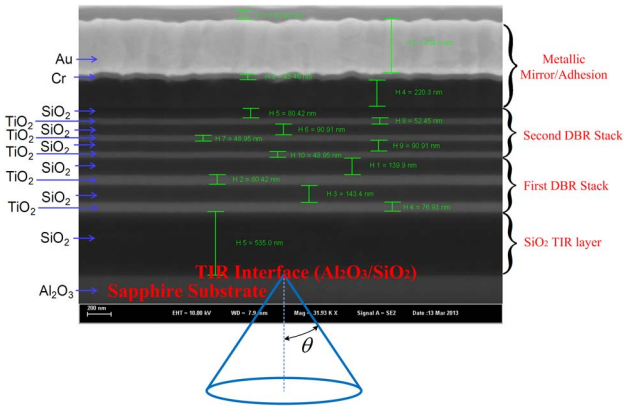

Fig. 8. SEM image of back hybrid reflector including SiO_2 TIR layer, five-pair double DBR stacks, and Au metallic mirror.

that is passing toward the hybrid reflector at angles greater than the critical angle (56°), while the light that passes through the SiO_2 TIR layer with incident angles between 0° and 56° are reflected by the double DBR stacks and Au metallic mirror.

The effect of different back reflectors on the luminous flux of pc-LEDs packaging modules was shown in Fig. 9. At 350 mA injection current, the luminous flux of pc-LED A (packaged LED chip with ten-pair SiO_2/TiO_2 single DBR stack), pc-LED B (packaged LED chip with ten-pair SiO_2/TiO_2 double DBR stacks), and pc-LED C (packaged LED chip with hybrid reflector consisting of five-pair SiO_2/TiO_2 double DBR stacks and Au metallic mirror) was 145.6 lm, 149.7 lm, and 150.8 lm, respectively. The higher luminous flux for pc-LED B and pc-LED C was attributed to the use of double DBR stacks, which exhibited high reflectivity in both the blue light wavelength and yellow light wavelength region. The higher reflectivity in yellow light wavelength region will benefit the pc-LEDs because yellow light backscattered by phosphor particles is reflected upward, resulting in an increase of luminous flux of pc-LEDs.

Moreover, the degradation of the pc-LEDs, as shown in Fig. 9, was also investigated based on high temperature/high humidity accelerated lifetime testing. The packaged LED samples (pc-LED A, pc-LED B, and pc-LED C) were placed in a humidity chamber that is controllable from room temperature to 100°C, and the packaged LED samples were then stressed at the condition of 85°C and 85% humidity using an injection current of 700 mA. The packaged LED samples were removed from the humidity chamber at specific intervals to measure the luminous flux. The intervals were fixed at 24 h, 48 h, 72 h, 120 h, and 168 h. After 168 h of temperature/humidity accelerated lifetime testing, the luminous flux of the pc-LED A decreased by 2.26% from 145.6 to 142.3 lm; the luminous flux of the pc-LED B decreased by 1.2% from 149.7 to 147.9 lm; the luminous flux of the pc-LED C decreased by 0.79% from 150.8 to 149.6 lm. Compared to pc-LED A and pc-LED B, the pc-LED C exhibited lower optical degradation.

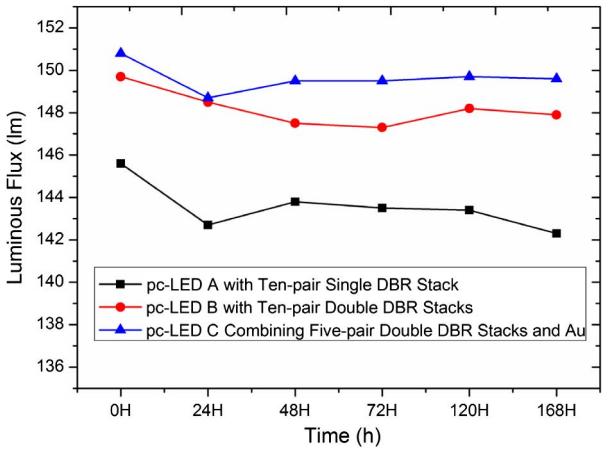

Fig. 9. Measured change in luminous flux of pc-LEDs with different back reflectors during the 168 h of temperature/humidity accelerated tests.

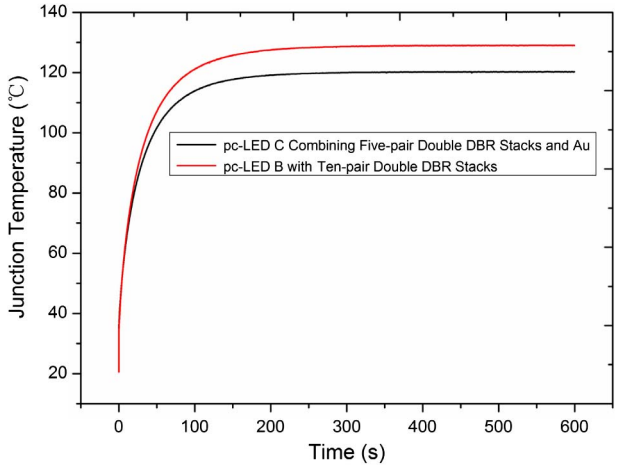

Fig. 10. Measured junction temperature of pc-LEDs with different back reflectors.

We used a T3Ster instrument (MicReD Inc., Hungary), which is a transient temperature measurement system and enables rapid and extremely accurate thermal characterization of LEDs to measure the junction temperature of pc-LEDs. Fig. 10 showed the measured junction temperature of pc-LEDs with different back reflectors. The measured junction temperature for pc-LED B and the pc-LED C was 128.9°C and 120.2°C, respectively. Compared to the LED B, the LED C with hybrid reflector combining five-pair SiO_2/TiO_2 double DBR stacks and Au demonstrated lower junction temperature due to the reduced number of SiO_2/TiO_2 pairs, leading to better heat spreading performance. The lower junction temperature can further improve the thermal reliability of pc-LED C, resulting in the lower optical degradation for pc-LED C during the 168 h of temperature/humidity accelerated lifetime testing, as shown in the above Fig. 9.

5. Conclusions

An LED chip with a hybrid reflector deposited on the bottom of the transparent sapphire substrate was fabricated. The back hybrid reflector, which offers metallic-like omnidirectional reflectivity together with frequency selectivity and low-loss behavior typical of a DBR, included a SiO_2 TIR layer, five-pair SiO_2/TiO_2 double DBR stacks, and an underlying layer of reflective metal. The double DBR stacks included a first DBR stack that was optimized for maximum reflection at 560 nm, and also included a second DBR stack that was optimized for maximum reflection at 460 nm. Compared to the single DBR stack, the high reflectivity for green, yellow, and red light as well as blue light can be obtained simultaneously using the double DBR stacks, which can further increase the luminous flux of the pc-LEDs and reduce the dependence of reflectivity on the angle of incidence.

This work was supported by the Project of the National Natural Science Foundation of China (No. 51305266).

References

1. M. S. Tsai, X. H. Lee, Y. C. Lo, and C. C. Sun, "Optical design of tunnel lighting with white light-emitting diodes," Appl. Opt. **53**, H114–H120 (2014).
2. P. Ge, Y. Li, Z. Chen, and H. Wang, "LED high-beam headlamp based on free-form microlenses," Appl. Opt. **53**, 5570–5575 (2014).
3. S. Zhou and S. Liu, "Transient measurement of light-emitting diode characteristic parameters for production lines," Rev. Sci. Instrum. **80**, 095102 (2009).
4. K. C. Huang, T. H. Lai, and C. Y. Chen, "Improved CCT uniformity of white LED using remote phosphor with patterned sapphire substrate," Appl. Opt. **52**, 7376–7381 (2013).
5. J. W. Pan, P. J. Tsai, K. D. Chang, and Y. Y. Chang, "Light extraction efficiency analysis of GaN-based light-emitting diodes with nanopatterned sapphire substrates," Appl. Opt. **52**, 1358–1367 (2013).
6. S. Zhou, B. Cao, S. Liu, and H. Ding, "Improved light extraction efficiency of GaN-based LEDs with patterned sapphire substrate and patterned ITO," Opt. Laser Technol. **44**, 2302–2305 (2012).
7. J. Z. Liu, M. D. B. Charlton, C. H. Lin, K. Y. Lee, C. Krishnan, and M. C. Wu, "Efficiency improvement of blue LEDs using a GaN burried air void photonic crystal with high air filling fraction," IEEE J. Quantum Electron. **50**, 314–320 (2014).
8. B. Cao, S. Li, R. Hu, S. Zhou, Y. Sun, Z. Gan, and S. Liu, "Effects of current crowding on light extraction efficiency of conventional GaN-based light emitting diodes," Opt. Express **21**, 25381–25388 (2013).
9. S. Zhou, B. Cao, S. Liu, and H. Ding, "High power GaN-based LEDs with low optical loss electrode structure," Opt. Laser Technol. **54**, 321–325 (2013).
10. H. Masui, N. N. Fellows, H. Sato, H. Asamizu, S. Nakamura, and S. P. DenBaars, "Direct evaluation of reflector effects on radiant flux from InGaN-based light-emitting diodes," Appl. Opt. **46**, 5974–5978 (2007).
11. D. X. Wang, I. T. Ferguson, and J. A. Buck, "GaN-based distributed Bragg reflector for high-brightness LED and solid-state lighting," Appl. Opt. **46**, 4763–4767 (2007).
12. Y. S. Zhao, D. L. Hibbard, H. P. Lee, K. Ma, W. So, and H. Liu, "Efficiency enhancement of InGaN/GaN light-emitting diodes with a back-surface distributed Bragg reflector," J. Electron. Mater. **32**, 1523–1526 (2003).
13. J. C. Su, C. L. Lu, and C. W. Chu, "Design and fabrication of white light emitting diodes with an omnidirectional reflector," Appl. Opt. **48**, 4942–4946 (2009).
14. D. Y. Kang, E. Wu, and D. M. Wang, "Modeling white light-emitting diodes with phosphor layers," Appl. Phys. Lett. **89**, 231102 (2006).
15. M. A. Kats, R. Blanchard, P. Genevet, and F. Capasso, "Nanometre optical coatings based on strong interference effects in highly absorbing media," Nat. Mater. **12**, 20–24 (2013).
16. T. X. Lee, K. F. Gao, W. T. Chien, and C. C. Sun, "Light extraction analysis of GaN-based light-emitting diodes with surface texture and/or patterned substrate," Opt. Express **15**, 6670–6676 (2007).
17. K. Wang, D. Wu, F. Chen, Z. Y. Liu, X. B. Luo, and S. Liu, "Angular color uniformity enhancement of white light-emitting diodes integrated with freeform lenses," Opt. Lett. **35**, 1860–1862 (2010).
18. R. Hu, X. Luo, and S. Liu, "Study on the optical properties of conformal coating light-emitting diode by Monte Carlo simulation," IEEE Photon. Technol. Lett. **23**, 1673–1675 (2011).
19. Z. Liu, S. Liu, K. Wang, and X. Luo, "Measurement and numerical studies of optical properties of YAG:Ce phosphor for white light-emitting diode packaging," Appl. Opt. **49**, 247–257 (2010).
20. Y. Fink, J. N. Winn, S. Fan, C. Chen, J. Michel, J. D. Joannopoulos, and E. L. Thomas, "A dielectric omnidirectional reflector," Science **282**, 1679–1682 (1998).
21. W. H. Southwell, "Omnidirectional mirror design with quarter-wave dielectric stacks," Appl. Opt. **38**, 5464–5467 (1999).
22. K. M. Chen, A. W. Sparks, H. C. Luan, D. R. Lim, K. Wada, and L. C. Kimerling, "SiO_2/TiO_2 omnidirectional reflector and microcavity resonator via the sol-gel method," Appl. Phys. Lett. **75**, 3805–3807 (1999).
23. Y. S. Huang, S. Y. Hu, C. C. Huang, Y. C. Lee, J. W. Lee, C. C. Chang, Z. K. Wun, and K. K. Tiong, "Incident-angle-dependent reflectance in distributed Bragg reflectors fabricated from ZnO/MgO multilayer films," Opt. Rev. **21**, 651–654 (2014).
24. A. Zukauskas, R. Vaicekauskas, F. Ivanauskas, H. Vaitkevicius, and M. S. Shur, "Spectral optimization of phosphor-conversion light-emitting diodes for ultimate color rendering," Appl. Phys. Lett. **93**, 051115 (2008).
25. S. J. Chang, C. F. Shen, M. H. Hsieh, C. T. Kuo, T. K. Ko, W. S. Chen, and S. C. Shei, "Nitride-based LEDs with a hybrid Al mirror + TiO_2/SiO_2 DBR backside reflector," J. Lightwave Technol. **26**, 3131–3136 (2008).
26. H. Guo, H. Chen, X. Zhang, P. Zhang, J. Liu, H. Liu, and Y. Cui, "High-performance GaN-based light emitting diodes on patterned sapphire substrate with a novel hybrid Ag mirror and atomic layer deposition TiO_2/Al_2O_3 distributed Bragg reflector backside reflector," Opt. Eng. **52**, 063402 (2013).
27. N. M. Lin, S. C. Shei, and S. J. Chang, "Nitride-based LEDs with high-reflectance and wide-angle Ag mirror + SiO_2/TiO_2 DBR backside reflector," J. Lightwave Technol. **29**, 1033–1038 (2011).
28. N. Thomas and J. Wolfe, "UV-shifted durable silver coating for astronomical mirrors," Proc. SPIE **4003**, 312–323 (2000).